ARTICLES

Surface States of Titanium Dioxide Nanoparticles Modified with Enediol Ligands

Linda de la Garza, Zoran V. Saponjic, Nada M. Dimitrijevic, Marion C. Thurnauer, and Tijana Rajh*

Chemistry Division, Argonne National Laboratory, 9700 South Cass Avenue, Argonne, Illinois 60439

Received: July 26, 2005; In Final Form: November 2, 2005

Control of surface states of titanium dioxide nanoparticles using 2-(3,4-dihydroxyphenyl)ethylamine (dopamine) and 3,4-dihydrophenylacetic acid, which act as ligands to the undercoordinated surface sites (carrier traps), is demonstrated by electrochemical techniques. The deepest traps were found to be most reactive and are selectively removed by the addition of the ligands which enhances the kinetics of electron accumulation in the film. Furthermore, a shift in the Fermi level to more positive potentials was detected for electrodes modified with the negatively charged ligand (3,4-dihydrophenylacetic acid) compared to that of electrodes modified with the positively charged ligand (dopamine). The presence of the negative charge on the ligand also contributed to the underpotential of hydrogen evolution on 3,4-dihydrophenylacetic acid-modified electrodes.

Introduction

The abrupt termination of the crystal units at the surface of metal oxide nanoparticles with a diameter of less than 10 nm gives rise to a different arrangement of the surface atoms compared to those in the bulk. The energy levels of these reconstructed surface species are found in the mid-gap region.[1] All surface states behave as donor or acceptor sites, and thus photogenerated charge carriers tend to be trapped at the surface of the semiconductor. Trapped electrons in TiO_2 nanoparticles and nanostructured TiO_2 films have been extensively studied.[2−6] Electron traps in TiO_2 are derived from native defects due to oxygen deficiencies and adsorbed species on the surface. These states result from the localization of an electron in the Ti 3d orbital.[7] However, the correlation of the structural deformations, energetics, and optical response of excess electrons trapped in bulk and surface trapping sites as well as conduction band (CB) electrons in TiO_2 nanoparticles is not entirely clear. To address these questions and to enhance and optimize charge-transfer dynamics, it is important to manipulate surface defects and trap states.[8−10] Our approach to achieve control of surface states is by selective modification of the surface of TiO_2 nanoparticles. In TiO_2 nanoparticles of about 45 Å diameter, the Ti atoms are pentacoordinated (square pyramidal) at the surface, whereas they are hexacoordinated (octahedral) in the bulk.[11] Enediol ligands, such as 2-(3,4-dihydroxyphenyl)ethylamine (dopamine), catechol, and 3,4-dihydroxyphenylacetic acid (dopac), have a large affinity for these under-coordinated surface sites, restoring the coordination of Ti atoms to the octahedral geometry and forming ligand-to-metal charge-transfer complexes.[12] Formation of these charge-transfer complexes on TiO_2 has been shown to enhance interfacial electron-transfer rates.[13,14] Enediol ligands used in this work selectively bind to the surface trapping sites and change the energetics of the surface states only. Therefore, by quantitatively modifying the surface with enediol ligands, the contributions of surface trapping states are selectively removed. Taking advantage of the specificity of enediol ligands for undercoordinated surface states, we characterized TiO_2 nanoparticulate films modified with dopamine (TiO_2/DA) and dopac (TiO_2/DC) using spectroelectrochemical techniques. Spectroelectrochemistry has been useful for obtaining a value for the flat band potential of nano-structured TiO_2 electrodes.[15−18] With this technique, the potential-dependent optical absorption spectral changes for nano-structured TiO_2 electrodes have been observed in two different ranges of electron accumulation, weak and strong. Under weak-accumulation conditions, surface and interior trapping states are filled by electrons, with the accumulated charges compensated by adsorption of protons or cations. Under strong-accumulation conditions, filling of the conduction band dominates, and the charge is compensated by intercalation of protons or cations.[19−21]

In this work, we used spectroelectrochemistry and cyclic voltammetry to analyze and characterize the changes in the energetics of the surface states due to the presence of the enediol ligands. It has been shown that surface states dominate interfacial electron-transfer dynamics as well as carrier mobility.[8−10] Spectroelectrochemical characterization of bare and ligand-modified TiO_2 nanoparticulate films was performed by a potentiostatic biasing electrode toward negative potentials. The applied potential increased the electron concentration in nanostructured TiO_2 films. As electrons accumulate in the film, they occupy the lowest energy states available. The difference of the absorption spectra before and after the applied potential provides a measure of the energetics of occupied electronic states. Changes in the absorption spectra of the film due to the accumulation of electrons can be spectroscopically monitored when indium tin oxide (ITO) is used as transparent back contact for TiO_2 films.

* To whom correspondence should be addressed. E-mail: Rajh@anl.gov.

10.1021/jp054128k CCC: $33.50
Published on Web 12/18/2005

Experimental Section

All the chemicals used were reagent grade and used without further purification. Nanopure water was used. The pH was adjusted using HCl and NaOH. Synthesis and characterization of TiO_2 nanoparticles have been described in detail previously.[12] Briefly, TiO_2 nanoparticles were synthesized by the dropwise addition of titanium(IV) chloride to cooled water. Slow growth of the particles was achieved using dialysis at 4 °C against water until the pH of the solution reached 3.5, when particle growth was complete (45 Å). Modified TiO_2 nanoparticles were prepared by addition of surface-active ligand (e.g. dopamine) to cover only a certain percentage of the nanoparticle surface.[12] Glass slides with a conductive side of indium tin oxide (ITO) ($R_s = 8-12\ \Omega$) from Delta Technologies were cleaned by 30 min sonication in a series of baths: 1:1 acetone/methanol, detergent, 20% sulfuric acid, 0.2 M NaOH in 1:1 water/methanol, and finally water. Nanoparticulate films of modified TiO_2 were prepared by dipping clean indium tin oxide slides in 0.13 M solution of TiO_2 having various dopamine coverage (from 0 to 50%). The slides were then dip-coated 3 times with drying in an oven at 150 °C for 30 min after each dip. The thicknesses of the resulting thin films were on the order of 100 nm.

Thermal gravimetric analysis (TGA) was performed on TiO_2/DA nanoparticles to investigate the stability of the ligand−TiO_2 complex under the conditions of electrode preparation. Tests showed that no changes other than water evaporation occurred below 150 °C. Dopamine oxidation was detected at temperatures higher than 250 °C. TGA measurements were obtained on a Seiko ExStar TG/DTA 6200 from Haake Instruments. The samples were measured against alumina standard in a 100 mL/min O_2 flow with temperature ramp of 5 °C/min to 600 °C.

The electrolyte for photoelectrochemical measurements was nitrogen-purged 40 mM phosphate buffer solution at pH 6.8 that contained hydroquinone as the redox relay. Photocurrents were measured with a Bioanalytical Systems Analyzer (BAS 100B) at 0 V vs Ag/AgCl (0.2 V vs NHE) reference electrode as the difference in current was observed with and without incident light on the backside of the ITO/TiO_2 film. Therefore, all potentials are reported vs Ag/AgCl electrode, unless otherwise stated. The counter electrode was a platinum wire; the electrochemical cell was a quartz cell of 10 mL volume. Monochromatic light was provided through a Jobin−Yvon grating monochromator in line with an ILC xenon arc lamp (300 W). The power density of the incident light was measured using a calibrated silicon diode detector (Ophir Optronics). Light intensity was ~0.5 mW/cm^2 at a 500 nm wavelength.

Cyclic voltammetry (CV) measurements of the TiO_2 electrodes were performed in nitrogen-purged 40 mM phosphate buffer solution at pH 6.8. A platinum wire was used as a counter electrode, and potentials were measured vs Ag/AgCl reference electrode using the BAS 100B.

Spectroelectrochemical measurements were performed with a Shimadzu UV−vis spectrophotometer with the cell compartment under nitrogen atmosphere. During these measurements a spectrophotometric cell containing about 3 mL of aqueous 0.2 M lithium perchlorate ($LiClO_4$) at pH 6.8 was used, the TiO_2 electrode was the working electrode, a Pt wire was the counter electrode, and the Ag/AgCl was the reference electrode.

Results and Discussion

Absorption Spectra of Ligand-Modified Nanoparticles. Addition of the surface-active molecules, both dopamine (DA) and dopac (DC), to a solution of TiO_2 nanoparticles produced an immediate change in the absorption spectra, indicating the formation of a charge-transfer complex. Surface titanium atoms are chelated by the enediol group of the ligands, and this interaction changes the electronic properties of the nanocrystalline particles.[12] The absorption spectrum of TiO_2 nanoparticles modified with increasing amounts (more surface coverage) of dopamine (TiO_2/DA) is shown in Figure 1. For bare TiO_2, the wavelength of onset of absorption is 380 nm, corresponding to a band gap of 3.2 eV for anatase.[22] Addition of dopamine on the TiO_2 surface shifts the onset of absorption to the visible range, where absorption, due to the charge-transfer complex, is observed (absorption threshold 800 nm). Increasing the amount of dopamine increases absorbance at all wavelengths <800 nm but does not shift the onset of absorption, leading to the effective band gap of dopamine-modified TiO_2 of 1.6 eV.[12]

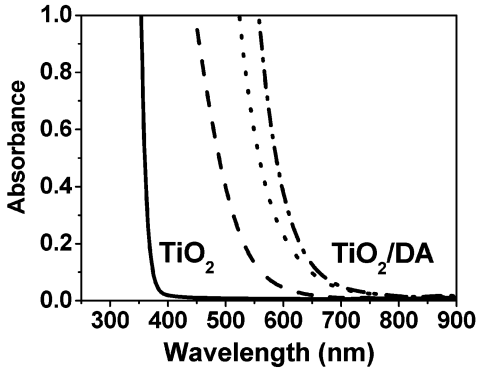

Figure 1. Absorbance spectrum for 0.13 M TiO_2 aqueous solution with 0% (solid), 5% (dash), 20% (dot), and 50% (dash dot) of the nanoparticle surface covered with dopamine (optical path 0.2 cm).

Photoelectrochemistry of Ligand-Modified TiO_2 Films. Nanocrystalline films were obtained from colloidal solution of TiO_2 nanoparticles modified with enediol ligands having 0%, 5%, 20%, and 50% of surface coverage. Surface trapping sites were eliminated in a controllable manner by increasing the amount of ligands. The absorption spectra of the films were measured before and after drying. No major changes were detected, indicating that the ligand-modified TiO_2 films were stable under the preparation conditions.

Photocurrent action spectra of ligand-modified films were measured and reflect the dependence of charge-transfer efficiency on the wavelength of absorbed light, as well as the electronic connectivity of the particles in the films. Absorption of light by the TiO_2/DA charge-transfer complex promotes electrons from the dopamine ligands to the conduction band of the TiO_2 particles and their subsequent collection by the conductive ITO substrate. The resulting photocurrent response (corrected for the lamp profile) for TiO_2 and TiO_2/DA films is shown in Figure 2. Collected electrons are measured as current during light−dark cycles obtained as square-shaped signals during the light cycles at different wavelengths of absorbed light (inset, Figure 2). The fast rise of the photocurrent (detection limit of the instrument is 50 ms) is indicative of efficient charge separation in the modified film as well as good electron donation from the redox relay in solution. The photocurrent produced by modified films reflects the absorption spectra, as can be seen by comparing Figures 1 and 2. For bare TiO_2 films, photocurrent production was mostly detected at wavelengths shorter than 400 nm, while for TiO_2/DA films photocurrent production starts in the visible range. This behavior indicates that the TiO_2/DA charge-transfer complex[12] is preserved in the film. The observed efficient charge separation in the film is a result of having

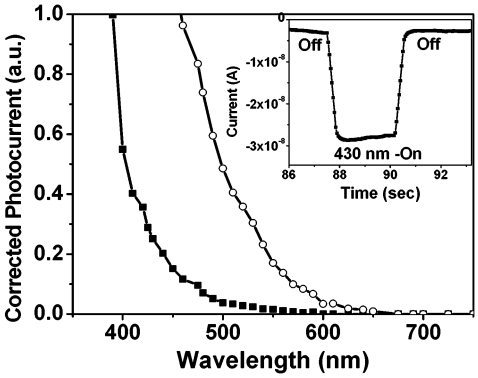

Figure 2. Corrected photocurrent action spectra of ligand-modified TiO_2 electrodes. Films with 0% (■) and 20% dopamine (○) on the surface of TiO_2 nanoparticles are shown. Inset: Current during an illumination cycle with 430 nm light for 20% TiO_2/DA electrode. 5 mM hydroquinone was the electron donor in 40 mM phosphate buffer pH 6.8, and Pt wire was the counter electrode.

good electric communication between TiO_2/DA particles and the film with the ITO substrate. The electric communication between the nanoparticles that constitute the film was maintained up to a surface coverage of 50%, at which a decrease of photocurrent was observed due to the lack of connectivity between nanoparticles. Similar photocurrent spectra were observed for TiO_2/DC films.

Spectroelectrochemistry and Cyclic Voltammetry of Ligand-Modified TiO_2 Films. Cyclic voltammetry is a technique of choice for detecting and characterizing surface traps in nanocrystalline electrodes. A shoulder in the current−potential curves of TiO_2 nanocrystalline electrodes that appears at potentials more positive than the potential of the CB edge has been generally assigned to the presence of electron traps.[2] In Figure 3a,b cyclic voltammograms of bare and ligand-modified TiO_2 films in the range of −0.35 to −1.0 V are presented. The conduction-band edge of TiO_2 at pH 6.8 is approximately at −0.67 V vs Ag/AgCl (−0.47 V vs NHE).[6] A feature at −575 mV in bare TiO_2 film corresponds to the filling of states below the conduction band edge, confirming the presence of surface traps.[3,19,23] After surface modification, the peak corresponding to reduction of the surface traps shifts to more negative potentials, and as the surface coverage increases to 50%, the peak reaches a potential close to the flat band potential (−0.67 V, Figure 3a). This shows that upon surface modification with enediol ligands, the deepest trapping sites are eliminated with the lower surface coverages, and as the concentration of ligand is increased, only shallow trap states are available. The deepest sites are most reactive toward bidentate ligands that repair the oxygen deficiency, and by controlling the amount of ligand, one can modulate the energetics of the surface states. The peak detected by cyclic voltammetry (in Figure 3a) shifts by approximately −100 mV for 50% surface coverage from the peak in bare TiO_2, which is in agreement with the previously reported changes in redox potential obtained by the electron-transfer reaction between methyl viologen and TiO_2/DA nanoparticles.[6] It is important to mention that for the same surface coverage, variation in film thickness or surface modifier (using DC instead of DA) did not change the surface trap reduction potential detected by cyclic voltammetry. As shown in Figure 3b, the surface trap reduction peaks appear at the same potential for 20% surface coverage for both DA and DC. The enediol group (HOC═COH) present in both ligands, namely dopamine and dopac, has the same affinity toward the under-coordinated Ti (defect sites), while their molecular structures differ only in the compositions of their pendent chains. It should be noted

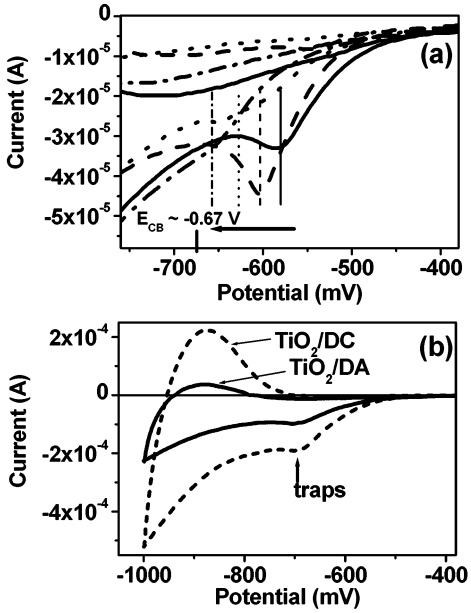

Figure 3. (a) Cyclic voltammograms of dopamine-modified TiO_2 electrodes. Scan rate = 5 mV/s. Films with 0% (solid), 5% (dash), 20% (dot), and 50% (dash dot) of dopamine on the surface of TiO_2 nanoparticles are shown. (b) Cyclic voltammograms of dopamine-(TiO_2/DA, solid) and 3,4-dihydroxyphenylacetic acid- (TiO_2/DC, dash) modified TiO_2 electrodes. Scan rate = 20 mV/s. Films with 20% of the surface of TiO_2 nanoparticles covered with ligands are shown.

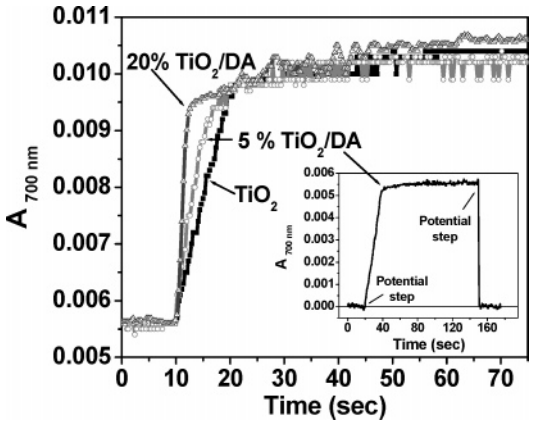

Figure 4. Absorbance at 700 nm of TiO_2 films with 0% (■), 5% (○), and 20% (△) of the nanoparticle surface covered with dopamine. Initial potential was −900 mV, and at 10 s the potential was changed to −950 mV. Inset shows the absorbance at 700 nm monitored for 5% dopamine surface coverage of the TiO_2 nanoparticle films during the application of a potential step. Initial potential was 0 mV, at 20 s, the potential was changed to −900 mV, and at 150 s the potential was changed back to 0 mV. All potentials vs Ag/AgCl.

that the voltage scan rate affects the current and slightly shifts the peak potential position (compare the peak position for 20% coverage in Figure 3a at 650 mV (5 mV/s) and the peak position for dopamine in Figure 3b at 680 mV (20 mV/s)). However, the trends obtained for the same scan rate (5 mV/s) were used to obtain relative energy differences between the surface states.

We examined the kinetics of the absorbance changes at 700 nm after applying a potential step for TiO_2 films having different nanoparticle surface coverage of the dopamine modifier. The absorbance signal increases with the step in potential and decreases to the original level when the potential is stepped back to the initial potential (inset Figure 4); thus the absorbance changes are reversible. The increase in absorbance was faster for the films having higher dopamine coverage, as shown in

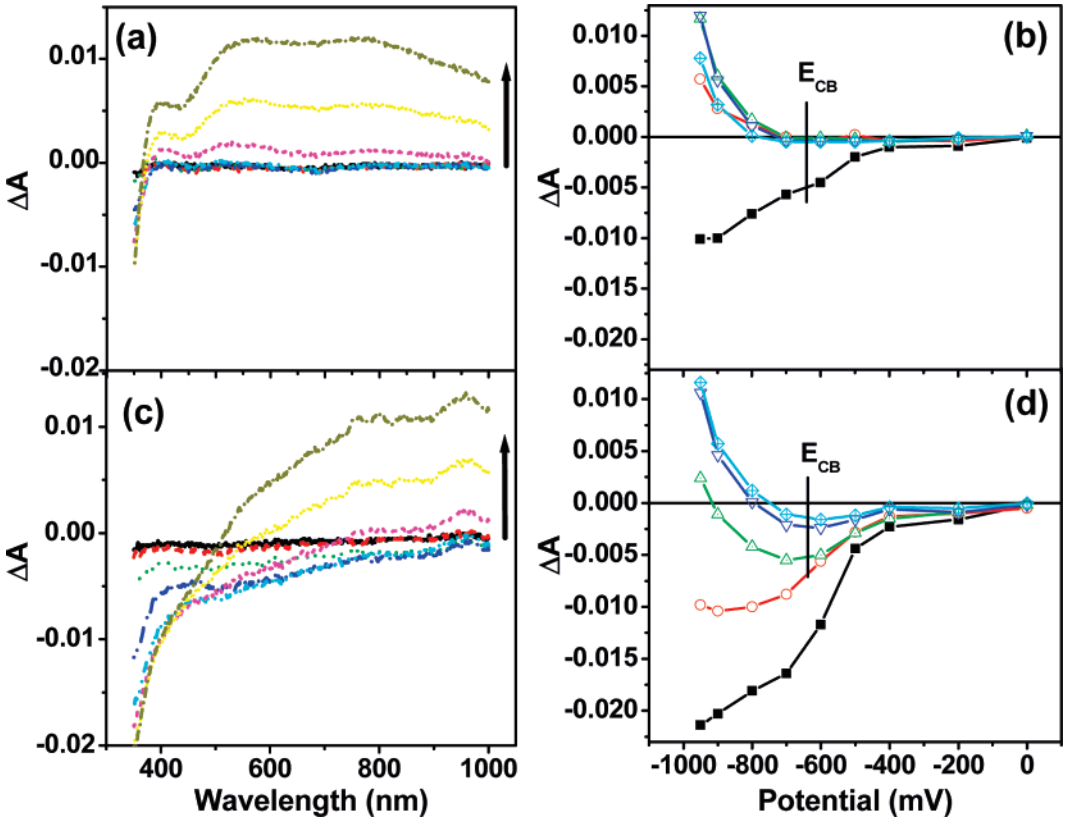

Figure 5. Spectra of TiO_2 films with 0% (a) and 50% (c) dopamine on the surface of TiO_2 nanoparticles measured at −200 mV (black), −400 mV (red), −500 mV (green), −600 mV (blue), −700 mV (light blue), −800 mV (pink), −900 mV (yellow), and −950 mV (dark yellow). The change in absorbance from (a) and (c) with applied potential is shown in (b) and (d), respectively. Wavelengths shown are 350 nm (■), 400 nm (○), 550 nm (△), 750 nm (▽), and 900 nm (◇).

Figure 4. The rise of the 700 nm absorbance with a potential step from −900 to −950 mV, corresponding to injection of electrons into the conduction band, is faster for the 20% > 5% > 0% TiO_2/DA films, leading to the initial rise in absorbance $\Delta A/s$ of 1.8×10^{-3} s^{-1} > 5.4×10^{-4} s^{-1} > 3.9×10^{-4} s^{-1} respectively. This observation indicates that electrons injected into TiO_2 are filling available conduction-band states faster when the surface of the particles is covered with 20% dopamine than when the surface does not have any ligand. These results suggest that eliminating the surface trapping sites leads to a higher mobility of electrons in TiO_2 nanoparticles, in agreement with the previous report that absence of trapping states results in higher mobility of electrons within oxides.[24]

To correlate the depth of different trapping sites with their optical properties, the absorbance changes in the series of ligand-modified nanostructured TiO_2 electrodes were monitored while maintaining potentiostatic control.[25−27] The absorption spectra between 350 and 1000 nm, measured at several applied potentials for bare TiO_2 and 50% surface-modified nanostructured TiO_2/DA films, are shown in Figure 5a and c, respectively. For bare TiO_2 film in Figure 5a, increase in absorbance is not apparent until potentials approaching the flat band potential (E_{fb} ∼ −0.67 V) are reached. However, slight bleaching of the absorption spectrum is detected even at the applied potentials more positive than the flat band potential, indicating that surface electrons can be excited to the conduction band and contribute to the filling of the bottom of the conduction band. Fitzmaurice and co-workers have reported spectroelectrochemical detection of surface states in bare TiO_2, with characteristic absorption at ∼400 nm appearing at potentials below the CB edge. We have not been able to detect this signal. One of the probable reasons of this discrepancy comes from the fact that their films are ∼10× thicker than the ones used in this work. Another is that energetic differences of surface states might arise from the fact that the particles used in their experiments are quite different from those used in this work, e.g., particle size and crystalline structure. The main spectral features obtained when the applied potential reaches the flat band potential are characteristic of trapped electrons, since the absorbance is higher in the visible range than in the near-infrared part of the spectrum. The observation of three different maxima at 400, 550, and 750 nm is indicative of the presence of at least three different localized states. In addition, a bleaching in the UV region (wavelengths shorter than 400 nm) is detected with negative bias. Figure 5b shows absorption changes with applied potential at different wavelengths. For all localized states (400, 550, and 750 nm) and free or shallow trapped electrons (900 nm), significant absorbance is detected only at potentials more negative than the flat band potential of −0.67 V.

The spectra from 50% of the surface-modified nanoparticulate TiO_2/DA film revealed entirely different behavior, shown in Figure 5c,d. The absorbance of TiO_2/DA electrodes at potentials more positive than the flat band potential is bleached, but at more negative potentials, the absorption spectra show complex behavior. The recorded change in absorption deconvolutes into two processes: one is the bleaching of the charge-transfer complex observed in the measurements involving injection of electrons at the potentials more positive than E_{fb}, and the second is the increase of the absorption due to the absorption of excess electrons. Initial biasing toward negative potentials, even below the flat band potential, causes a bleaching at wavelengths shorter than 900 nm that can be assigned to the bleaching of the charge-transfer complex absorption. Excitation of electrons occupying surface states is enough to bleach the charge-transfer complex

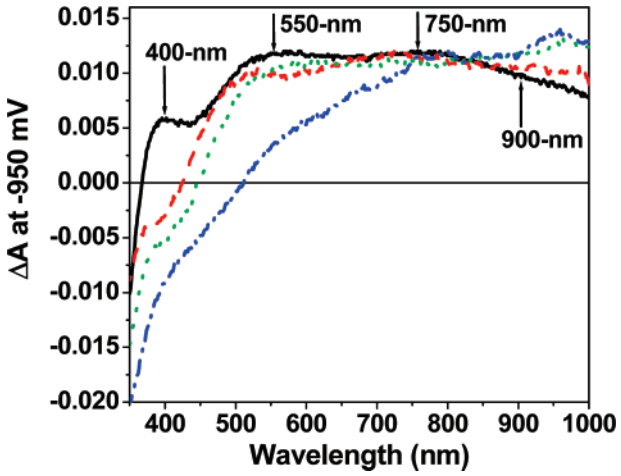

Figure 6. Spectra of TiO_2 films with 0% (black), 5% (red), 20% (green), and 50% (blue) of dopamine on the surface of nanoparticles measured at −950 mV potential in 0.2 M $LiClO_4$.

absorption, which occurs at lower photon energies than the absorption from bare TiO_2. Even when a 900 nm probe light excites electrons from the surface states to the conduction band it causes a bleaching of the TiO_2/DA absorption due to the weak absorption of the charge-transfer complex in the IR region that cannot be resolved in the absorption spectrum (Figure 1). It should be pointed out that sensitive detection of a bleach in the charge-transfer complex absorption is possible due to its large oscillator strength and, therefore, high extinction coefficient (ϵ) of the charge-transfer complex absorption[12] compared to that of trapped electrons in bare TiO_2.[13]

The contribution of the absorption of excess electrons to the overall changes in the absorption spectrum becomes more apparent after applied potentials reach E_{fb} because of the low extinction coefficient and small oscillator strength of trapped and free carriers compared to the extinction coefficient of the charge-transfer complex. As described previously, trap carriers show preferential optical transitions with energies in the visible region while free carriers show a continuous rise of absorption toward lower energies (proportionally to λ^2).[28] In our experiments, at applied potentials more negative than E_{fb}, the absorption of excess electrons is detected only at the longer wavelengths (750 and 900 nm) while at 350 nm, bleaching of the CT complex exceeds the absorption of excess electrons (−0.5 V) as shown in Figure 5d.

Spectral features of excess electrons allow investigation of their nature and changes that occur upon surface modification. For this purpose, spectra obtained for different surface coverage of TiO_2/DA nanoparticulate films were normalized and are shown in Figure 6. The increase in surface coverage by dopamine changes the shape of the spectra, indicating the changes in the energetics of surface states. At 0 and 5% of surface coverage, broad maxima are observed, while at 20 and 50% the spectra flatten and do not decrease at longer wavelengths. However, the shapes of the spectra do not follow the λ^2 dependence expected for free electrons. By simple examination of the shape of the spectra at the higher negative potentials, it is reasonable to say that electrons in surface-modified films have less trapped character than the ones in bare TiO_2. We find that 5% coverage of DA eliminates the localized state associated with absorption maximum at 400 nm. Concomitantly, using CV, we found that the broad peak for surface-trapped electrons centered at −575 mV is shifted to −600 mV (Figure 3). Correlating these two measurements we find that the majority of the deepest trapped carriers that absorb at 400 nm have the redox potential of −575 mV. Similarly, we find that those surface trapping sites that absorb at 550 nm are correlated to the redox potential of −625 mV. With 50% surface coverage only shallow trapping sites that absorb in the IR remain (Scheme 1).

SCHEME 1: Salient Features of the Electronic Structure of 4.5 nm TiO_2 Particles upon Surface Modification with Different Concentration of Dopamine[a]

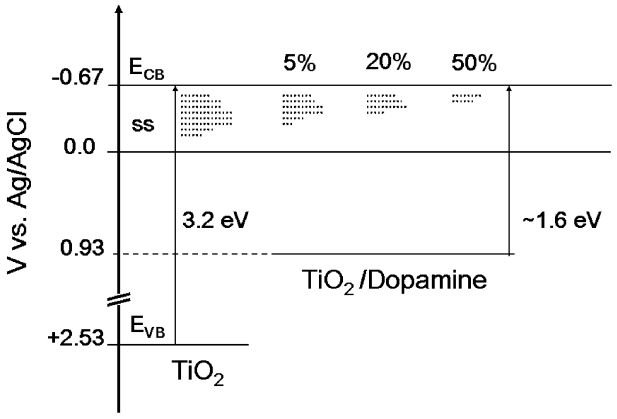

[a] Upon surface modification the deepest surface sites (SS) are removed by using the smallest concentration of dopamine, suggesting that the deepest sites are the most reactive toward bidentate binding. Upon modification of 50% of surface sites only the shallow surface sites remain.

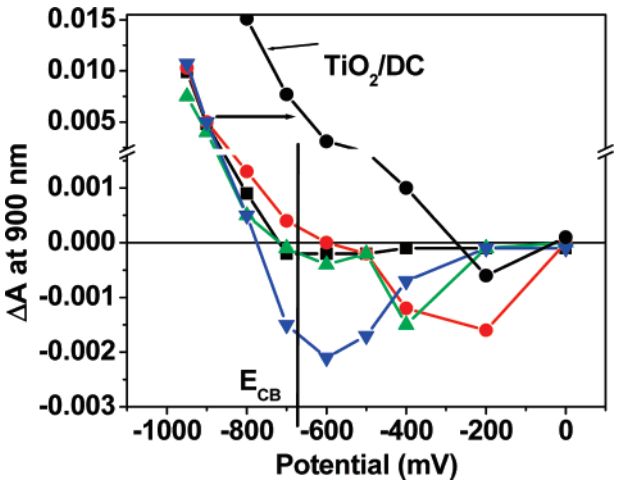

Figure 7. Absorbance change at 900 nm for TiO_2 films with 0% (■), 5% (○), 20% (△), and 50% (▽) of the nanoparticle surface covered with dopamine. Absorbance change at 900 nm for TiO_2 film 5% (◇) of the nanoparticle surface covered with 3,4-dihydroxyphenylacetic acid (TiO_2/DC) is also shown.

Another, more direct way of correlating the spectral changes with the energy of injected electrons (applied potential) is obtained by plotting the change in absorbance vs applied potential for the series of ligand-modified TiO_2 films as shown in Figure 7. We have chosen absorbance at 900 nm because at this wavelength both the CT complex and the CB electrons absorb light. Moreover, at 900 nm, the absorption of excess electrons is equal to the bleaching of the CT complex (for the maximum coverage of 50%) at flat band potential (Figure 5d), indicating that their extinction coefficients at this wavelength are comparable. As demonstrated previously, applying to the film a potential more positive than the flat band potential, such as −200 mV, results in occupation of surface states that can be promoted into the CB and causes the bleaching of the hybrid complex. Two processes contribute to the overall absorption. The first process is a decrease of absorption (bleaching) due to

the promotion of electrons from surface states to the CB, caused by an apparent increase of the band gap of the hybrid particle. However, when an appreciable amount of surface electrons is reached, a positive change in the absorbance is detected. Figure 7 clearly shows that absorption by surface states is present at different potentials for each surface-modified film. For 5% TiO_2/DA film, the onset of absorption occurs at −200 mV reaching a maximum at −575 mV, for 20% TiO_2/DA film the onset of absorption occurs at −400 mV reaching a plateau at −600 mV, and for 50% TiO_2/DA film the onset occurs at −600 mV while the maximum is now located within the CB absorbance. These measurements are reminiscent of the CV curves and reflect the change in the energetics of the surface states upon their chemical modification. The results indicate that, at 5% coverage, the energy of surface states is fairly broad and is -575 ± 375 mV, and for 20% coverage, the energy of surface states is -600 ± 200 mV, suggesting that there is a shift of the energy of surface states closer to the conduction band with a narrowing of their distribution. A schematic representation of the processes contributing to this complex behavior of surface-modified electrodes is given in Scheme 1 showing that the deep trapping sites localized at lower energies are eliminated by increasing the amount of ligand leaving only shallow traps when the surface coverage of 50% is achieved. Once the applied potential reaches E_{fb}, there are no other major differences with respect to the bare TiO_2.

The same approach was used to investigate the effect of the charge of the surface-active molecules on the redox properties of the nanoparticle. When 3,4-dihydroxyphenylacetic acid (5% TiO_2/DC), a negatively charged analogue of dopamine, was used as surface-active species, the absorption spectra at potentials between 0 and −500 mV were very similar to those of 5% TiO_2/DA. However, at potentials more negative than −500 mV, the positive absorption continuously builds up in contrast to bare and dopamine-modified TiO_2 films, for which the onset of absorption occurs at potentials more negative than −700 mV. That is, accumulation of electrons in 3,4-dihydroxyphenylacetic acid-modified films occurs at significantly lower potential than in dopamine-modified films, indicating that the presence of a negative charge on the enediol-type surface modifier (DC) causes a shift of the flat band potential toward more positive values. While dopamine is an amine-terminated ligand ($pK = 8.87$)[29] with a positive charge at pH 6.8, 3,4-dihydroxyphenylacetic acid bears a carboxylic acid that is deprotonated at the same pH ($pK = 4.2$).[30] The positive charge of the dopamine pendent group repels positive protons from the surface of nanocrystalline films. On the other hand, the negative charge in TiO_2/DC films causes a high concentration of protons to accumulate around the surface of the modified nanoparticles, producing the same effect as decreasing the pH. Therefore, the high local concentration of protons will alter the position of flat band potential according to the Nernst equation:

$$E_{fb} = E_{fb}(\text{pH } 0) - 0.059\,[\text{pH}] = E_{fb}(\text{pH } 0) + 0.059 \log[H^+_{loc}] \quad (1)$$

where E_{fb}(pH 0) is the flat band potential at pH 0 and $[H^+_{loc}]$ is the local concentration of protons. To confirm the existence of the double-layer effects resulting in the shift of the flat band potential in DC-modified electrodes at pH 6.8, we measured the open circuit voltage of DC- and DA-modified electrodes. The open circuit measurements showed that the flat band potential of DC-modified electrodes is ∼120 mV more positive than DA-modified electrodes in the dark, as well as upon illumination under the same experimental conditions, confirming that the charge of the adsorbed ligands can cause double-layer effects that can be used to alter the flat band potential of nanocrystalline electrodes.

As a consequence of the double-layer effects, the same chemical reactions occur at different potentials for differently charged electrodes. In TiO_2/DC-modified films the accumulation of electrons was easily released at −0.6 V at pH 6.8 by the production of a gaseous product, while in TiO_2/DA films the same process occurs at potentials of −1.0 V. Concomitantly, the initial bleach in TiO_2/DC films at 350 nm, due to accumulation of electrons in the CB, recovers at potentials more negative than −0.6 V, suggesting that electrons are being consumed in the reduction of H^+ to produce H_2. This interpretation is supported by the existence of a high local concentration of adsorbed H^+ that can cause underpotential for hydrogen evolution. A larger accumulation of electrons saturates the film, and the disappearance of electrons that absorb at 900 nm was detected at potentials more positive than −0.8 V. The overpotential for hydrogen evolution was eliminated even though the driving force for H^+ reduction for TiO_2 and TiO_2/DA films is larger than for TiO_2/DC due to the apparent differences in CB energetics.

Conclusions

The surface properties of TiO_2 nanoparticles modified by enediol ligands have been studied by electrochemical and spectroelectrochemical methods. Optical detection of the surface traps is possible due to the high extinction coefficient of the charge-transfer complex. Measurement of the dependence of the absorbance change with applied potential in surface-modified films directly reports on the energetics and distribution of surface trapping sites. The measurements indicate that the most reactive sites, and the first to be restructured and removed by binding of the enediol ligands, are the deepest trapping sites. Upon surface modification, the energy of surface sites shifts toward the energy of CB states and their distribution narrows. In addition, manipulation of the surface charge of TiO_2 nanoparticles using surface-active ligands was found to kinetically enhance a desired chemical reaction and gives rise to the underpotential for hydrogen evolution.

Acknowledgment. This work was supported by the U.S. Department of Energy, Office of Basic Energy Sciences, Division of Chemical Sciences, Geosciences and Biosciences, under contract W-31-109-Eng-38. L.d.l.G. and M.C.T. acknowledge Argonne National Laboratory for support.

References and Notes

(1) Gutierrez, C.; Salvador, P. *J. Electroanal. Chem.* **1982**, *138*, 457−463.
(2) Wang, H.; He, J.; Boschloo, G.; Lindstrom, H.; Hagfeldt, A.; Lindquist, S. E. *J. Phys. Chem. B* **2001**, *105*, 2529−2533.
(3) Boschloo, G.; Fitzmaurice, D. *J. Phys. Chem. B* **1999**, *103*, 2228−2231.
(4) Boschloo, G.; Goossens, A.; Schoonman, J. *J. Electroanal. Chem.* **1997**, *428*, 25−32.
(5) Szczepankiewicz, S. H.; Moss, J. A.; Hoffmann, M. R. *J. Phys. Chem. B* **2002**, *106*, 7654−7658.
(6) Dimitrijevic, N. D.; Saponjic, Z. V.; Bartels, D. M.; Thurnauer, M. C.; Tiede, D. M.; Rajh, T. *J. Phys. Chem. B* **2003**, *107*, 7368−7375.
(7) Cao, F.; Oskam, G.; Searson, P. C.; Stipkala, J. M.; Heimer, T. A.; Farzad, F.; Meyer, G. J. *J. Phys. Chem.* **1995**, *99*, 11974−11980.
(8) Boschloo, G. K.; Goossens, A. *J. Phys. Chem.* **1996**, *100*, 19489−1949.
(9) Huber, R.; Spörlein, S.; Moser, J. E.; Grätzel, M.; Wachtveitl, J. *J. Phys. Chem. B* **2000**, *104*, 8995−9003.
(10) Gregg, B. A.; Chen, S. G.; Ferrere, S. *J. Phys. Chem. B* **2003**, *107*, 3019−3029.

(11) Rajh, T.; Nedeljkovic, J. M.; Chen, L. X.; Poluektov, O.; Thurnauer M. C. *J. Phys. Chem. B* **1999**, *103*, 3515−3519.
(12) Rajh, T.; Chen, L. X.; Lukas, K.; Liu, T.; Thurnauer, M. C.; Tiede, D. M. *J. Phys. Chem. B* **2002**, *106*, 10543−10552.
(13) Redmond, G.; Fitzmaurice, D.; Grätzel, M. *J. Phys. Chem.* **1993**, *97*, 6951−6954.
(14) Moser, J.; Punchihewa, S.; Infelta, P, P.; Grätzel, M. *Langmuir* **1991**, *7*, 3012−3018.
(15) O'Regan, B.; Grätzel, M.; Fitzmaurice, D. *Chem. Phys. Lett.* **1991**, *183*, 89−93.
(16) O'Regan, B.; Grätzel, M.; Fitzmaurice, D. *J. Phys. Chem.* **1991**, *95*, 10525−10528.
(17) Rothenberger, G.; Fitzmaurice, D.; Grätzel, M. *J. Phys. Chem. B* **1992**, *96*, 5983−5986.
(18) Kavan, L.; Grätzel, M. *Electrochim. Acta* **1995**, *40*, 643−652.
(19) Kavan, L.; Kratochvilova, K.; Grätzel, M. *J. Electroanal. Chem.* **1995**, *394*, 93−102.
(20) Boschloo, G.; Fitzmaurice, D. *J. Electrochem. Soc.* **2000**, *147*, 1117−1123.
(21) Fabregat-Santiago, F.; Mora-Seró, I.; Garcia-Belmonte, G.; Bisquert, J. *J. Phys. Chem. B* **2003**, *107*, 758−768.
(22) Hagfeldt, A.; Grätzel, M. *Chem. Rev.* **1995**, *95*, 49−68.
(23) Kavan, L.; Grätzel, M.; Rathousky, J.; Zukal, A. *J. Electrochem. Soc.* **1996**, *143*, 394−400.
(24) Hao, E.; Anderson, N. A.; Asbury, J. B.; Lian, T. *J. Phys. Chem. B* **2002**, *106*, 10191−10198.
(25)) Kolle, U.; Moser, J.; Grätzel, M. *Inorg. Chem.* **1985**, *24*, 2253−2258.
(26) Dimitrijevic, N. M.; Savic, D.; Micic, O. I.; Nozik, A. J. *J. Phys Chem.* **1984**, *88*, 4278−4283.
(27)) Safrany, A.; Gao, R.; Rabani, J. *J. Phys. Chem. B* **2000**, *104*, 5848−5853.
(28)) Pankove, J. I. *Optical Processes in Semiconductors*; Prentice-Hall: Engelwood Cliffs, NJ, 1971; p 74.
(29) Antikainene, P. J.; Witikainen, U. *Acta Chem. Scand*. **1973**, *27*, 2075.
(30) Turkel, N.; Berker, M.; Ozer, U. *Chem. Pharm. Bull*. **2004**, *52*, 929.